

# Reduction of Damage of Buried Ammunition Depots in the Ground by Crumb Rubber Cement against Explosion Force

Mehdi Mirzaee<sup>1</sup>, Mostafa Vaezi<sup>2</sup>✉, Saeid Mamandi<sup>3</sup> and Omid Abdolrahman<sup>3</sup>

<sup>1</sup>Faculty of Engineering, Tarbiat Modares University, Tehran, Iran

<sup>2</sup>Department of Maritime Engineering, Amir Kabir University, Tehran, Iran

<sup>3</sup>Faculty of Engineering, Islamic Azad University, Mahabad Branch, Iran

✉Corresponding author's Email: mvaezi7067eng@aut.ac.ir

**ABSTRACT:** Nowadays, due to the development of missiles with high power of destruction and accuracy as well as the increase in terrorist attacks, it is better to keep military equipment in the depth of the ground. Using the underground structures (US) has been interested in shelters and ammunition depots for many years. But these structures should also be resistant to surface explosions. For this purpose, the structure must be constructed at high depths or the structure protected by the specific coating. The aim of this study was introduced and evaluates the performance of a combined coating containing crumb rubber cement (CRC) to prevent the transmission of compression waves. Hence, to check the effectiveness of this coating by modeling a buried structure in ANSYS LS-DYNA at a depth of 5 meters from the ground surface and placing crumb rubber cement CRC at a depth of 2 meters from the ground surface and above the structure, the model was subjected to an explosion equivalent to 100 kilograms of TNT was analyzed for 25 milliseconds. The results showed that by inserting crumb rubber cement CRC, because of high elasticity with large deformations of crumb rubber (CR), adding it into concrete can absorb energy and reduce its transfer to the Layers down, and therefore lead to a reduction in the amount of failure and pressure which applies to the structure. To investigating the effect of the thickness of the CR layer, the pressure, and failure rate of the structure was analyzed for 0.1, 0.2, 0.3, 0.4, 0.5 m thickness layers. The results indicated that by increasing the thickness of the CR from 0.1 m to 0.5 m, the pressure and failure rate is reduced. But the intensity of this decrease of 0.4 meters later is very low so that it can be ignored. It is concluded that, CR with a thickness of 0.4m with concrete cover can be considered as a recommended optimal design and an applicable strategy in the construction of buried structures on the ground against the explosion forces.

**Keywords:** Ammunition depots, Crumb rubber, Concrete cover, Explosion, TNT

## INTRODUCTION

Various structures ranging from coastal structures to buried concrete depots, as one of the strategic structures, play a significant role in the military and economic purposes of a country, which should be given special attention to their reinforcement. Accordingly, the optimum design of structures such as coastal structures, concrete structures have been among the main concerns of many researchers (Pourzangbar et al., 2016, 2017a, 2017b; Pourzangbar, 2012; Yeganeh-Bakhtiary et al., 2015; Vaezi et al., 2016a, b).

Conducting passive defense measures in today's wars to confront enemy invasions and mitigate the

damage caused by land, air, and naval attacks is a fundamental issue that broadly covers all key infrastructures, vital and important military and civilian centers in the country (Amir et al., 2017).

Passive defense is one of the most effective and stable defense against threats has always been the focus of most countries in the world. These structures should also be resistant to surface explosions. Therefore, it is important to identify and investigate the parameters that affect the performance of these structures and increase the safety of these structures (Feldgun et al., 2011). A lot of research has been carried out on this subject, that in the below some of them being mentioned. Feldgun et al. (2011) presented a comprehensive approach to simulating

ORIGINAL ARTICLE  
 PII: S225204301800004-8  
 Received 07 Feb. 2018  
 Revised 25 Feb. 2018  
 Accepted 01 Mar. 2018

the distribution of explosive pressure on a flexible or hard flat barrier in porous soils. Yang and Wang (2006) investigated the effect of air blast on surface structures with regard to Shock in the soil. In this research, he also used the LS-DAYNA finite element software and modeled the soil into a three-phase mode equation. Lu and Wang (2006) presented a model for nonlinear dynamical analysis of explosion and distribution of pressure of it in the soil. They have modeled by using non-linear analysis of LS-DYNA software and an appropriate state equation and behavioral model for materials, soil, explosives, and structures in an environment. Naghizadeh et al. (2010) performed numerical modeling of the effect of the surface explosion on buried structures. They also used a model similar to the model provided by Lu and Wang for modeling of geometry. Gholizadeh and Rajabi (2013) in addition to studied the effects of surface and subsurface blast on buried structures and their modeling, they have also predicted strategies for improving the safety of these structures and their efficiency.

In this study, to prevent the transmission of pressure waves from the explosion through the soil, and consequently, to reduce the damage of buried ammunition depots, a special cover CRC is evaluated. The reason for using this coating is the high elasticity of the rubber in absorption and damping the energy of surface explosions. We will study first the modeling of the LS-DYNA finite element software, and then introduce the geometric shape of the model and finally, the results of the research are discussed.

## MATERIAL AND METHODS

### Numerical modeling in LS-DYNA software

In this study, the LS-DYNA software was used to model, analyze and evaluate the results. This software uses the finite element method. In this study, the structure and surrounding soil are modeled in 2-D. In the following, the equations of the states and the properties of the materials used to model the soil, structure, air and explosion phenomenon will be investigated, and then the geometric of the model with dimensions of modeling is presented. In the end, the results will be examined.

### Explosion

The explosion is characterized by the sudden and rapid release of sound a large amount of energy, producing light, heat, sound, and wave at speeds around the speed of sound (Ngo et al., 2007).

When an explosion occurs, the energy is released suddenly in a very short time (several milliseconds), and the effect of this energy release is seen in the form of thermal radiation and the propagation of compressive waves in space.

As a result of the explosion, the gas pressure is formed, which increases with the release of the explosion source and increases to a maximum positive PSO+ pressure, and then decreases to an ambient pressure Which this phase is called positive phase. As a result of the wave propagation, the gases produced by the explosion are cooled down and pressures are slightly less than atmospheric pressure. Because of this pressure difference, it is reversed to the center of the explosion. The result will be a reduction in pressure or suction which is called a negative phase. The negative phase suction is relatively small and gradual so that it is often neglected to design explosion-resistant structures. The maximum pressure from the explosion (PSO+) significantly decreases when it is away from the explosion center (Corresponding to the third power to the explosion center), but contrary to that, the loading period (the time of the load caused by the explosion on the structure) increases with the increasing distance from the explosion center (Figure 1) (UFC, 2008).

The TNT element was used to model the explosion by using the Jones-Wilkins-Lee (JWL) equation. This model is widely used that in which the pressure caused by the explosion is defined by (Eq. 1) (Wang et al., 2005).

$$P = A \times \left(1 - \frac{w\rho}{R_1\rho_0}\right) \times e^{\left(-R_1\frac{\rho_0}{\rho}\right)} + B \times \left(1 - \frac{w\rho}{R_2\rho_0}\right) \times e^{\left(-R_2\frac{\rho_0}{\rho}\right)} + \frac{w\rho^2}{\rho_0} E_{m0} \quad (1)$$

In which A, B, R1, R2, and w are the material constants. Parameters of  $\rho_0$  and  $\rho$  are the initial density and the product density of the explosion process respectively. The initial ratio of the  $\rho/\rho_0$  is considered equal to one. The parameter of  $E_{m0}$  is the Primary energy. The parameters of (Eq. 1) are given in (Table 1) (Wang et al., 2005).

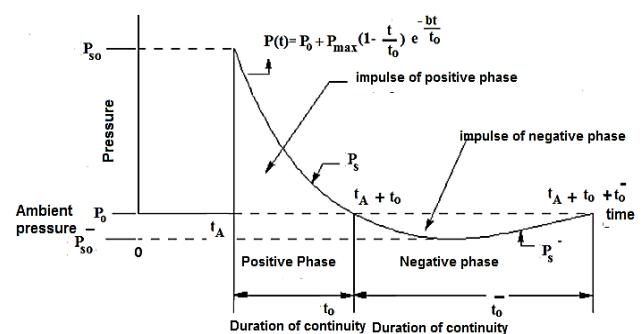


Figure 1. Diagram of pressure-time wave explosion

Table 1. Parameters related to JWL

Parameter	C (m/s)	Energy/vol (KJ/m3)	pressure (MPa)	Em0 (KJ)	
Value	6930	6e6	2.1e4	3.681e6	
Parameter	A (MPa)	B (MPa)	R1	R2	W
Value	3.737e5	3.747e3	4.15	0.9	0.35

## Soil

The soil used in this study is sandy clay (10% sand) that surrounds the structured environment. For modeling the soil against the explosive load it is necessary to consider its state equation. In this study, based on Fiserova's research (Fiserova 2005-2006), a compaction state equation for Sandy clay has been used. This equation

is calibrated based on the explosion loading rate and its results have been tested and approved by the TM5-855-1 and laboratory results (Leong et al., 2007). Also, MO Granular and Failure model were used to consider the soil-resistance behavior and the failure model. The parameters of the equation of state and resistance behavior are given in Tables 2 and 3.

**Table 2.** Parameters of the dense state equation -linear

Density parameter (g/cm <sup>3</sup> )	$\rho_1$	$\rho_2$	$\rho_3$	$\rho_4$	$\rho_5$	$\rho_6$	$\rho_7$	$\rho_8$	$\rho_9$	$\rho_{10}$
Value	1.674	1.740	1.847	1.997	2.144	2.25	2.38	2.485	2.585	2.6713
Pressure parameter (MPa)	$P_1$	$P_2$	$P_3$	$P_4$	$P_5$	$P_6$	$P_7$	$P_8$	$P_9$	$P_{10}$
Value	0	4.577	14.98	29.1	59.1	98.1	179.4	290	450.2	650.7
Density parameter (g/cm <sup>3</sup> )	$\rho_1$	$\rho_2$	$\rho_3$	$\rho_4$	$\rho_5$	$\rho_6$	$\rho_7$	$\rho_8$	$\rho_9$	$\rho_{10}$
Value	1.674	1.746	2.086	2.15	2.3	2.57	2.598	2.635	2.641	2.8
Sound speed (m/s)	$v_1$	$v_2$	$v_3$	$v_4$	$v_5$	$v_6$	$v_7$	$v_8$	$v_9$	$v_{10}$
Value	265.2	852.1	1721.7	1875.5	2264.8	2956	3112	4600	4634	4634

**Table 3.** Parameters of strength model - MO Granular

Pressure parameter (MPa)	$\rho_1$	$\rho_2$	$\rho_3$	$\rho_4$	$\rho_5$	$\rho_6$	$\rho_7$	$\rho_8$	$\rho_9$	$\rho_{10}$
Value	0	3.4	35	101.3	184	500	0	0	0	0
Yield stress (MPa)	$\sigma_{Y1}$	$\sigma_{Y2}$	$\sigma_{Y3}$	$\sigma_{Y4}$	$\sigma_{Y5}$	$\sigma_{Y6}$	$\sigma_{Y7}$	$\sigma_{Y8}$	$\sigma_{Y9}$	$\sigma_{Y10}$
Value	0	4.23	44.6	124	226	226	0	0	0	0
Density parameter (g/cm <sup>3</sup> )	$\rho_1$	$\rho_2$	$\rho_3$	$\rho_4$	$\rho_5$	$\rho_6$	$\rho_7$	$\rho_8$	$\rho_9$	$\rho_{10}$
Value	1.674	1.74	2.086	2.15	2.3	2.57	2.598	2.635	2.641	2.8
Shear modulus (MPa)	$G_1$	$G_2$	$G_3$	$G_4$	$G_5$	$G_6$	$G_7$	$G_8$	$G_9$	$G_{10}$
Value	76.9	869	4030	4900	7770	14.8e3	16.5e3	36.7e3	37.3e3	37.3e3

## Wave propagation in the soil

The propagation of the waves caused by the explosion in the soil in two forms: the volumetric (pressure) and the surface wave (Riley), which the most destructive of these is the pressure wave for a buried structure close to the explosion site. The propagation of this wave in continuous and free environments can be calculated by (Eq. 2, Eq. 3) (Lu et al. 2005):

$$u = 160f_c \frac{(2.52R/1)^{-n}}{w^3} \quad (2)$$

$$p_g = \rho.C.u \quad (3)$$

Where  $f_c$  is the coefficient of connection between the ground and explosive,  $w$  is the explosive mass to Kg,  $R$  is the distance from the explosion to meter,  $C$  is the velocity of the explosion wave in meters per second,  $P$  pressure in soil to kg / m<sup>2</sup>,  $\rho$  is the density Soil to kg/m<sup>3</sup> and  $n$  is the soil parameters that can be calculated from TM5-855-1 (Wang et al. 2005).

## Concrete

For concrete modeling, the P-alpha equation (Herrmann, 1969) and RHT resistance model are used to describe the deviation results of concrete. The P-alpha

equation is suitable for explicit dynamic analysis and provides accurate behavior of materials in high stresses. The RHT model is an advanced model for plastic material behavior that is designed for brittle materials by Riddle et al (1999). This model is especially useful for modeling concrete with dynamic loading. This model is also suitable for modeling brittle materials such as rocks and ceramics. The strength model uses three strength surfaces (Figure 2) an elastic limit surface, a failure surface and the remaining strength surface for the crushed material. Usually, there is a cap on the elastic strength surface.

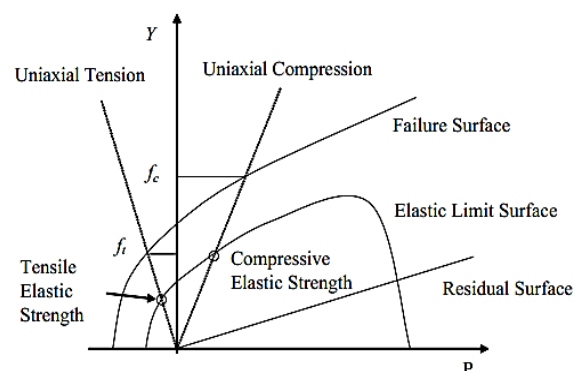


**Figure 2.** Three strength surfaces for concrete (Lu et al., 2005)

Following the hardening phase, additional plastic straining of the material leads to damage and strength reduction. Damage is accumulated by (Eq. 4, Eq. 5).

$$D = \sum \frac{\Delta \varepsilon_{pl}}{\varepsilon_p^{failure}} \quad (4)$$

$$\varepsilon_{pd}^{failure} = D_1 (p^* - p_{spall}^*)^{D_2} \geq \varepsilon_f^{min} \quad (5)$$

Where D1 and D2 are damage constants,  $\varepsilon_f^{min}$  is the minimum strain to reach failure,  $\varepsilon_{pl}$  and  $p^*$  is the pressure normalized by  $f_c$ , and  $p_{spall}^* = p^* (f_t/f_c)$  where  $f_t$  and  $f_c$  are tensile and compressive strength, respectively. Tables 4 and 5 shows the parameters used for the P-Alpha equation and the RHT resistance model Respectively:

**Table 4.** Parameters of the state equation- P-Alpha

Parameter	Porous dens (g/cm3)	Ref. dens (g/cm3)	Porous sound speed (m/s)	Init. Com. pr. (KPa)	Sol. Com. Pr. (KPa)
Value	2.314	2.75	2.92e3	23.3e3	6e6
Parameter	n	A1 MPa	A2 MPa	A3 MPa	B1,B2 -
Value	3	35.27e3	39.58e3	904e4	1.22

**Table 5.** Parameters of strength model - RHT

Parameter	Shear modul. (Mpa)	fc (Mpa)	ft/fc -	fs/fc -	A -
Value	16.7e3	35	0.1	0.18	1.6
Parameter	N	Q	Brit. To Duc. Trans.	Gelas/Gplas	Elas. Stre./ft
Value	0.61	0.68	0.0105	2	0.7
Parameter	Elas. Stre./fc	B	M	Com. Stre. Exp	Tens. Stre. Exp.
Value	0.53	1.6	0.61	0.032	0.036
Parameter	D1	D2	$\varepsilon_{f,min}$	-	-
Value	0.04	1	0.01	-	-

### Reinforcement steel bar

The steel 1006, with a linear equation and the Johnson-Cook resistance model, were used with regard to the failure due to the strain of the plastic (Autodyn help, 2005). The Johnson-Cook model is a rate dependent, elastic-plastic model. The model defines the yield stress Y by (Eq. 6) (Autodyn help, 2005).

$$Y = [Y_0 + B \cdot \varepsilon_p^n][1 + C \log \varepsilon_p^*][1 - T_H^m] \quad (6)$$

Where  $Y_0$  is the initial yield strength,  $\varepsilon_p$  is the effective plastic strain,  $\varepsilon_p^*$  is the normalized effective plastic strain rate, B,C,n, m are material constants.  $T_H$  is homologous temperature,  $T_H = (T - T_{room}) / (T_{melt} - T_{room})$  with  $T_{melt}$  being the melting temperature and  $T_{room}$  the ambient temperature. The parameters of the linear equation and the reinforcing resistance model are given in (Table 6).

### Atmosphere

Ideal gas state equation was used to model the air around the model. This equation is one of the simplest

state equations for ideal gases, which has been used in many applications that include gas movement. This equation is defined as (Eq. 7).

$$P = (\gamma - 1) \rho \cdot e \quad (7)$$

Where  $\gamma$ ,  $\rho$  and  $e$  Are adiabatic exponent, density and special air temperature. The parameters of (Eq.7) are given in Table 7.

**Table 6.** Linear Equation and Johnson-Cook Resistance Model

Parameter	Shear yield (Mpa)	Yield Stre. (Mpa)	Hard. Cons -	Hard. Exp. -	Strat.Rat. Cons. -
Value	81.7e3	350	275	0.36	0.022
Parameter	Ref. Strat. Rat.	Ultimate Plastic Strain			-
Value	1	0.2			-

**Table 7.** Parameters of the ideal gas state equation

Parameter	$\gamma$ -	Ref. Dens. (g/cm <sup>3</sup> )	Ref. Temp. (K)
Value	1.4	1.225e-3	288.2

### Crumb rubber (CR)

For CR modeling, rubber element with mechanical properties of NBR rubber was used with state equation and hyperelastic resistance model (Autodyn help, 2005, Pornprasit et al., 2016). This equation is suitable for modeling materials with high strain range. There are several models in the hyperelastic resistivity model for solving the problem. In this study, we used the Ogden model. The Ogden model is suitable for materials with a range of strain energy potentials of over 700% (Autodyn help, 2005). Due to the high rubber capability in energy absorption, this model is suitable. The strain energy potential of the Ogden model is defined as Eq. (8): (Autodyn help, 2005):

$$\begin{aligned} \psi = & \frac{\mu_1}{\alpha_1} (\lambda_1^{\alpha_1} + \lambda_2^{\alpha_1} + \lambda_3^{\alpha_1} - 3) \\ & + \frac{\mu_2}{\alpha_2} (\lambda_1^{\alpha_2} + \lambda_2^{\alpha_2} + \lambda_3^{\alpha_2} - 3) \\ & + \frac{\mu_3}{\alpha_3} (\lambda_1^{\alpha_3} + \lambda_2^{\alpha_3} + \lambda_3^{\alpha_3} - 3) \\ & + \frac{1}{d_1} (J-1)^2 + \frac{1}{d_2} (J-1)^4 + \frac{1}{d_3} (J-1)^6 \end{aligned} \quad (8)$$

Where  $\psi$  strain energy potential  $\lambda_p$  and  $J$  are deviatoric principal stretches of the left-Cauchy -Green tensor and determinant of the elastic deformation gradient respectively.  $\mu_p$ ,  $\alpha_p$  and  $d_p$  are material constants. In (Tables 8 and 9), the parameters used for the Hyperelastic state equation and Hyperelastic-Ogden 3rd Order strength model are expressed.

**Table 8.** Parameters of Hyperelastic state equation

Parameter	Ref. Dens. (g/cm <sup>3</sup> )
Value	1

**Table 9.** Parameters of Hyperelastic-Ogden 3rd Order strength model

Parameter	Mu1 (Kpa)	Alpha1	d1 (1/Kpa)	Mu2 (Kpa)	Alpha2
Value	5	1.18	4.82e-6	1.3	618.03
Parameter	d2 (1/Kpa)	Mu3 (Kpa)	Alpha3	d3 (1/Kpa)	-
Value	0	-9.81	-2	0	-

### Boundary condition of the model

In this study, the flow-out and transmission elements were used to create a semi-infinite environment and to prevent the return of the explosive pressure waves. These elements provide the pass of flow and materials from the boundaries of the model. The flow out element was used at the boundaries of the space around the model to

transmit air pressure and the transmission element was used around the soil environment.

### Geometric of the model

For modeling of concrete structures, soil, explosives, and air were used from Lagrangian, ALE and Eulerian, respectively. The model used consists of three parts: structure, soil, air. The explosive is equivalent to 100 kilograms of TNT. Figure 3 shows a graphical representation of the modeling geometry in the software.

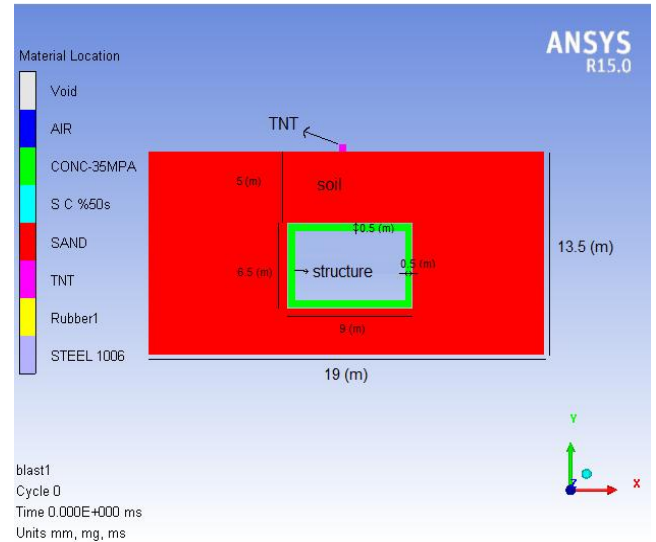


**Figure 3.** Modeling geometry in the software

### Sensitivity analysis

To test the sensitivity of the results to the size of mesh, the pressure output at a depth of 3 meters from the soil surface was compared for different sizes of the mesh (Figure 4). As shown in Figure 4, with a reduction in the size of the elements from 0.5 m to 0.1 m, significant changes are made to the results. On the other hand, by reducing the size of the elements from 0.125 meters later, the output pressure is very small and can be ignored. So the mesh size of 0.125 m was chosen as the optimal mesh.

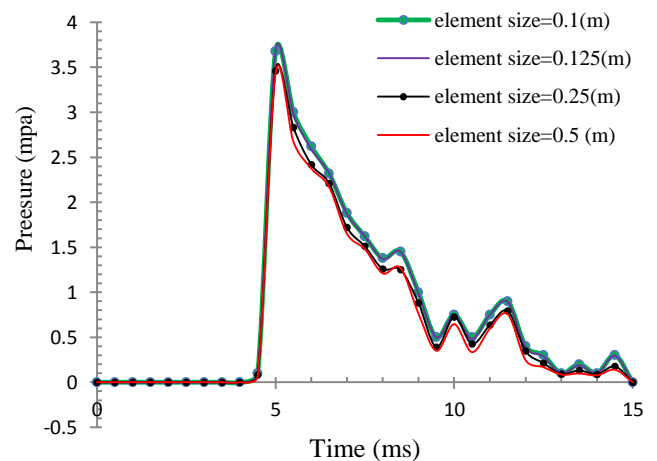


**Figure 4.** Variations of Pressure vs. time for different sizes of elements

## RESULTS AND DISCUSSION

### Distribution of wave explosion in the soil

To investigate the propagation of the wave explosion in the soil and the pressure at different depths, gauges were placed at depths of one meter at a distance. Figure 5 shows the pressure against time at depths of 1 and 2 meters from the soil surface for 25 milliseconds of analysis.

Figure 5 showed that the intensity of the pressure caused by the explosion has been reduced by increasing the distance from the soil surface (the explosion site).

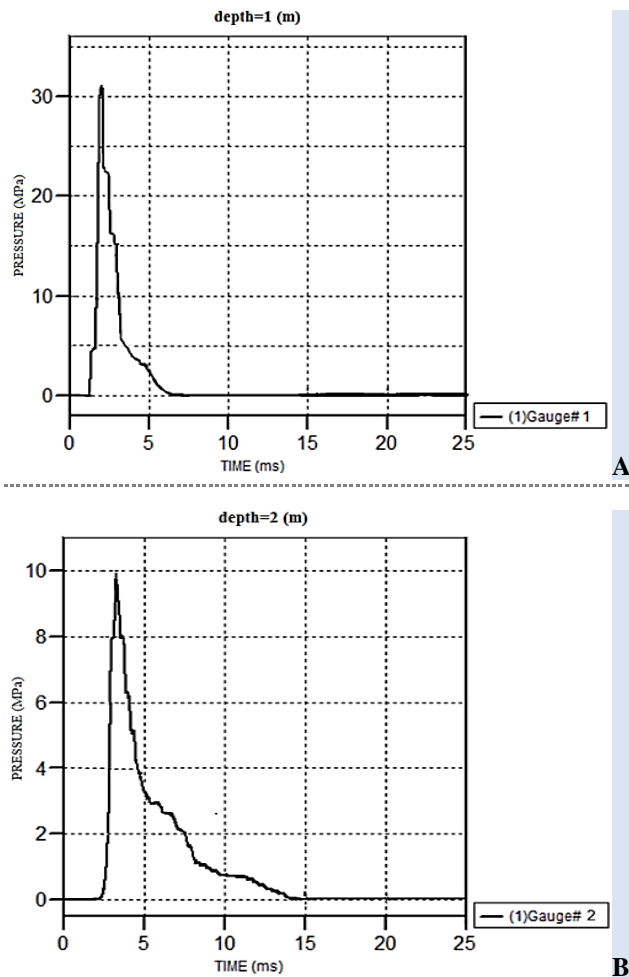


**Figure 5.** Pressure diagrams in soil A: At a depth of 1 meter from the ground B: At a depth of 2 meters from the ground

### Impact of crumb rubber cement (CRC) on results

In order to investigate the effect of CRC on the results, by modeling concrete cover and CR at a depth of 2 m from the ground surface and by comparing the results of pressure at a depth of 3 m (under the sub-layer of CR in the presence and absence of these layers effect these layers were examined. Figure 6 illustrated the graphic failure of the structure in the presence and absence of CR and concrete cover.

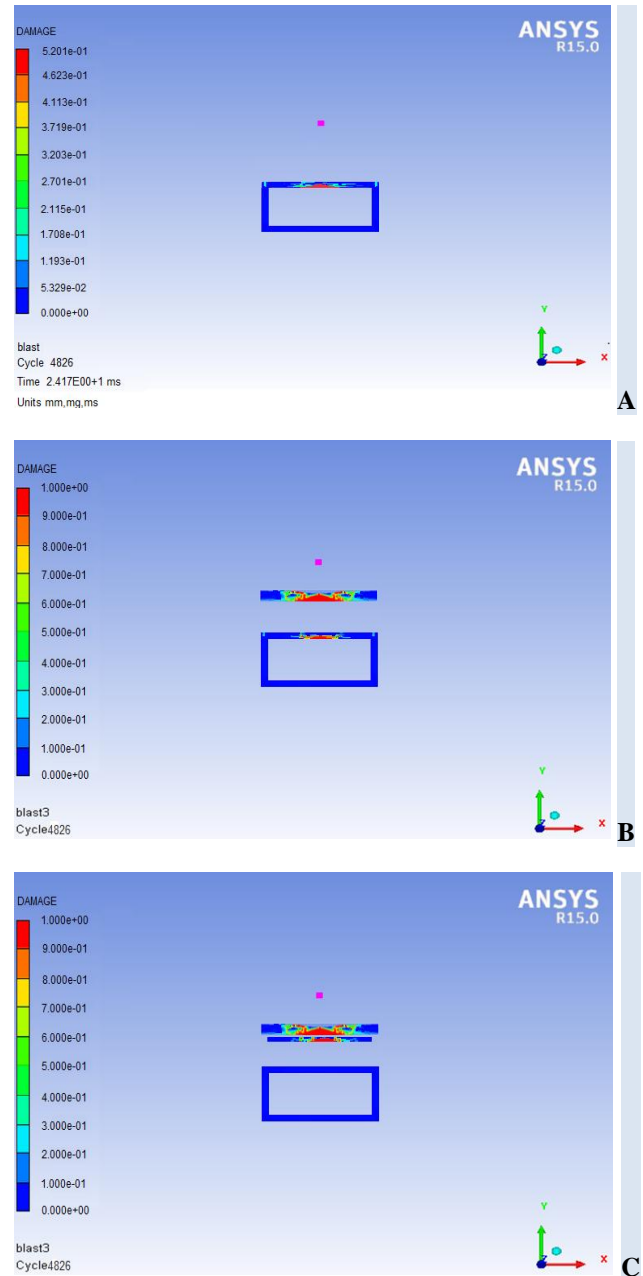


**Figure 6.** Graphical pattern of failure in model A: in the absence of concrete cushions and rubber substrates; B: in the presence of concrete cushions and no substratum; C: in the presence of rubber substrates and concrete cushions

Also, to investigate the effect of the protective layer CRC pressure and failure at a depth of 3 m below the protective layer were measured at gauge No. 3 at different times. The pressure and failure variations diagram at a depth of 3 meters and above the structure are shown in Figures 7 and 8 for different states of the CR substrate.

As shown in Figures 7 and 8, the presence of a single concrete cover only has a very small effect on the results. While modeling of CR has achieved significant changes in the number of results. On the other hand, the amount of pressure and damage decreases with the increase in the thickness of the CR layer. Also, according to the results, it can be seen that the reduction of pressure

and damage is a slight decrease after 0.4 m thickness. Therefore, the thickness of 0.4 m can be determined as optimal thickness.

In order to check the accuracy of maximum explosion pressure, using the (Eq. 2, Eq. 3) and also the parameters of Table 10 (TM5-855-1, 1984), the maximum value of the pressure from the results of the software is compared with the experimental results as follows.

As can be seen in table 10, the maximum value of the pressure from the experimental relation is conservative, which can be due to the linearity of the equation.

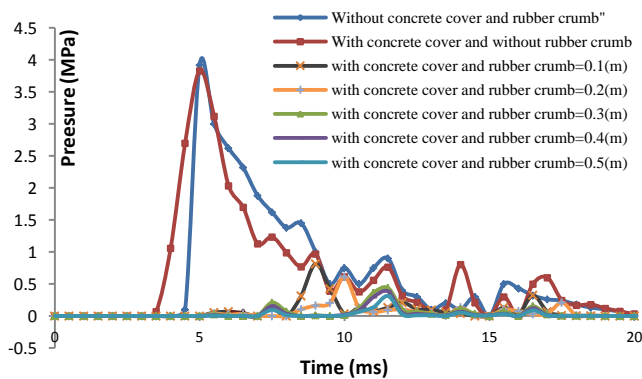


**Figure 7.** Pressure changes vs. time in different modes of existence and absence of (CR) and concrete cover at a depth of 3 meters

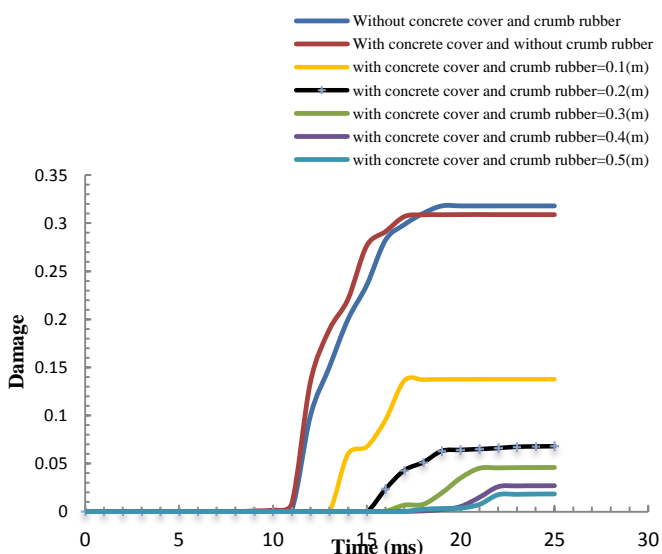


**Figure 8.** Failure diagram vs. time in different modes of existence and absence of CR and concrete cover on top of the structure

**Table 10.** The experimental parameters of the TM-5-855-1 instructions to calculate the pressure caused by the explosion at a distance of 3 meters

Soil type	Connection factor	W	R	Scaled distance	n	$\rho$	C	$P_{max}$
	-	(Kg)	(m)	-	-	(Kg/m <sup>3</sup> )	(m/s)	(Mpa)
Sand clay	0.4	100	3	0.4	2.4	1670	549	4.53

## CONCLUSION

In this study, the effect of crumb rubber cement (CRC) on reducing the amount of failure and pressure caused by the explosion phenomenon was investigated. Therefore, the geometric model of the structure and its surrounding soil, as well as the explosion phenomenon, was analyzed in the LS-DYNA finite element software. The results showed that despite the CR and with an increase in the thickness of the CR layer, the amount of the failure and pressure applied to the structure caused by the explosion wave is greatly reduced. But this reduction is very small and can be ignored after 0.4 meters in thickness. Therefore, 0.4 m thickness of the CR was selected as the optimum thickness of the CR layer to control the failure and pressure.

According to the results of this research, it can be seen that the reason for the high performance of the crumb rubber in absorption and damping of energy is its high elasticity. Therefore, high-elasticity polymeric materials can be used to absorb more energy.

## DECLARATIONS

### Authors' contribution

All authors contributed equally to this work.

### Competing interests

The authors declare that they have no competing interests.

## REFERENCES

- Amir SD, sahman S, hesam K. (2017). A modal nonlinear static analysis method for assessment of structures under blast loading. *Journal of Vibration and Control*, 64: 124-137.
- Feldgun V.R, Karinski Y.S, Yankelevsky D.Z.z. (2011). Blast Pressure Distribution on a Buried Obstacle in a Porous Wet Soil. *Journal of Vibration and Control*, 2: 45-69.
- Lu Y, Wang Z. (2006). Characterization of Structural Effects from Above-Ground Explosion Using Coupled Numerical Simulation. *Comput. Struct*, 84: 1729- 1742.
- Lu Y, Wang Z, Chong K. (2005). A comparative study of buried structure in soil subjected to blast load using 2D and 3D numerical simulations. *Soil Dynamics and Earthquake Engineering*, 25: 275–288.
- Nagy N, Mohamed M, Boot J. C. (2010). Nonlinear Numerical Modeling for the Effects of Surface Explosions on Buried Reinforced Concrete Structures. *Geomechanics and Eng., an Int. J. Techn*, 2: 1- 18.
- Amin G, Mohsen R. (2013). Secure concrete structures buried against the explosive load. *Scientific Journal of Passive Defense Science and Technology*, 3: 167-179.
- Ngo T, Mendis P, Gupta A. (2007). Blast loading and blast effects on structures—an overview.

- Electronic Journal of Structural Engineering, 7: 76–91.
- Department of Defense, Unified facilities criteria. 2008. Structures to resist the effects of accidental explosions, UFC, 3: 340-02.
- Wang Z.Q, Lu Y, Hao H, Chong K. (2005). A full coupled numerical analysis approach for buried structures subjected to subsurface blast. *Comput. Struct*, 83(4-5): 339-356.
- Fiserova D. (2005-2006). Numerical Analyses of Buried Mine Explosions with Emphasis on Effect of Soil Properties on Loading. Cranfield University.
- Leong E.C, Anand S, Cheong H.K, Lim C.H. (2007). Re-examination of peak stress scaled distance due to ground shock. *International Journal of Impact Engineering*, 34: 1487-1499.
- Herrmann W. (1969). Constitutive Equation for the Dynamic Compaction of Ductile Porous Materials, *J. Appl. Phys*, 40 (6): 2490-2499.
- Riedel W, Thoma K, Hiermaier S, Schmolinske E. (1999). Penetration of Reinforced Concrete by BETA-B-500, Numerical Analysis using a New Macroscopic Concrete Model for Hydrocodes. *Internationales Symposium, Interaction of the Effects of Munitions with Structures, Berlin Strausberg, 03.-07: 315 – 322.*
- Autodyn help. (2005). Theory Manual. Century Dynamics INS: Revision.
- Pornprasit R, Pornprasit P, Boonma P, Natwichai J. (2016). Determination of the Mechanical Properties of Rubber by FT-NIR, *Journal of Spectroscopy*. 247-255.
- Pourzangbar A. (2012). Determination the most effective parameters on scour depth at seawalls using genetic programming (GP). The 10<sup>th</sup> international conference on coasts. Ports and marine structures (ICOPMASS 2012). Tehran. Iran (Oral presentation).
- Pourzangbar A, Saber A, Yeganeh-Bakhtiary A, Rasoul Ahari L. (2016). Predicting Scour Depth at Seawalls using GP and ANNs. *Journal of Hydroinformatics*, 19(2).
- Pourzangbar A, Brocchini M, Saber A, Mahjoobi J, Mirzaaghahi M, Barzegar M. (2017). Prediction of scour depth at breakwaters due to non-breaking waves using machine learning approaches. *Journal of Applied Ocean Research*, 68: 120-128.
- Pourzangbar A, Losada M.A, Saber A, Rasoul Ahari L, Larroudé F, Vaezi M, Brocchini M. (2017). Prediction of non-breaking wave-induced scour depth at the trunk section of breakwaters using Genetic Programming and Artificial Neural Networks. *Journal of Coastal Engineering*, 121: 107-118.
- Vaezi M, Pourzangbar A, Fadavi M, Rahbar Rangi A. (2016). Configuration effects on the performance of viscous dampers (Text in Persian). 4<sup>th</sup> International Congress on Civil Engineering Architecture and Urban Development 27-29 December 2016, Shahid Beheshti University. Tehran. Iran (Oral presentation).
- Vaezi M, Pourzangbar A, Fadavi M, Rahbar Rangi A. (2016). Impact of different configurations and increasing difficulty bracing elements in viscous damper performance. The 18<sup>th</sup> Marine Industries Conference (MIC2016). Kish Island. Iran (Oral presentation).
- TM5-855-1. 1984. Fundamental of protective design for conventional weapons. US Army Engineer Waterways Experiment Station, Vicksburg.
- Yeganeh-Bakhtiary A, Pourzangbar A, Hajivalie F. (2015). Genetic Programming to predict scour depth at coastal structures. *Journal of Civil and Environmental Engineering*, 45(78): 115-122.